Identification of Multiple Amyloidogenic Sequences in Laminin-1†

Shingo Kasai,[‡,§] Shunsuke Urushibata,[‡] Kentaro Hozumi,[||] Fumiharu Yokoyama,[§] Naoki Ichikawa,[§] Yuichi Kadoya,[⊥] Norio Nishi,[§] Nobuhisa Watanabe,[@] Yoshihiko Yamada,[||] and Motoyoshi Nomizu*[,‡]

Tokyo University of Pharmacy and Life Science, Tokyo 192-0392, Japan, Division of Bioscience, Graduate School of Environmental Earth Science, Hokkaido University, Sapporo 060-0810, Japan, Craniofacial Developmental Biology and Regeneration Branch, National Institute of Dental and Craniofacial Research, National Institutes of Health, Bethesda, Maryland 20892-4370, Department of Anatomy, Kitasato University School of Medicine, Sagamihara 228-8555, Japan, and Division of Biological Sciences, Graduate School of Science, Hokkaido University, Sapporo 060-0810, Japan

Received October 9, 2006; Revised Manuscript Received February 3, 2007

ABSTRACT: Amyloid fibril formation is associated with several pathologies, including Alzheimer's disease, Parkinson's disease, type II diabetes, and prion diseases. Recently, a relationship between basement membrane components and amyloid deposits has been reported. The basement membrane protein, laminin, may be involved in amyloid-related diseases, since laminin is present in amyloid plaques in Alzheimer's disease and binds to amyloid precursor protein. Recently, we showed that peptide A208 (AASIKVAVSADR), the IKVAV-containing peptide, formed amyloid-like fibrils. We previously identified 60 cell adhesive sequences in laminin-1 using a total of 673 12-mer synthetic peptides. Here, we screened for additional amyloidogenic sequences among 60 cell adhesive peptides derived from laminin-1. We first examined amyloid-like fibril formation by the 60 active peptides with Congo red, a histological dye binding to many amyloid-like proteins. Thirteen peptides were stained with Congo red. Four of the 13 peptides promoted cell attachment and neurite outgrowth like the IKVAV-containing peptide. The four peptides also showed amyloid-like fibril formation in both X-ray diffraction and electron microscopic analyses. The amyloidogenic peptides contain consensus amino acid components, including both basic and acidic amino acids and Ser and Ile residues. These results indicate that at least five laminin-derived peptides can form amyloid-like fibrils. We conclude that the laminin-derived amyloidogenic peptides have the potential to form amyloid-like fibrils in vivo, possibly when laminin-1 is degraded.

The process of amyloid fibril formation is associated with several diseases, including Alzheimer's disease, Parkinson's disease, type II diabetes, prion diseases, and systemic polyneuropathies (*1*, *2*). Many proteins not associated with amyloid-related diseases can also form amyloid-like fibrils (*3*−*5*). Although they contain distinct protein sequences (*6*), the amyloid-like fibrils have similar structural properties and exhibit a red to green birefringence after staining with Congo red (*7*, *8*). Amyloid fibrils have a cross-β conformation and are on average 7−10 nm in diameter and variable length. Amyloid fibril formation is different from the simple process of nonspecific aggregation because it has ordered structures that possess a characteristic X-ray diffraction pattern (*6*, *9*). Thus, a specific pattern of molecular interactions, rather than nonspecific hydrophobic interactions, leads to ordered structures. Common structural elements responsible for such organized structures have not been identified.

Basement membrane components have been identified in amyloid plaques from Alzheimer's patients (*10*, *11*). Basement membranes are thin extracellular matrices that play a critical role in tissue structural support, filtration, development, repair, tumor growth, and metastasis. Laminins, major glycoprotein components of basement membranes, promote the biological functions of the basement membrane (*12*). Laminins are trimeric molecules composed of α, β, and γ chains. So far, five α, three β, and three γ chains have been identified which assemble to form 15 identified isoforms. Laminin-1 ($\alpha1\beta1\gamma1$) has diverse biological activities, including promotion of cell adhesion, migration, neurite outgrowth, tumor metastasis, and angiogenesis (*12*). Laminin-1 and the $\gamma1$ chain are overexpressed in glial cells and accumulate punctately in plaques of Alzheimer's brain. In addition, immunohistochemical analysis of Alzheimer's brain tissue reveals that the β-amyloid peptide and overexpressed laminin $\alpha1$ chain are colocalized in senile plaques (*13*). Previous studies demonstrate that laminin-1 and its degraded fragments interact with β-amyloid peptides, inhibit neurotoxicity, and disrupt amyloid fibril formation in vitro (*14*, *15*). We previously found that an Ile-Lys-Val-Ala-Val (IKVAV)-

† This work was supported by Grants-in-Aid for Scientific Research from the Ministry of Education, Culture, Sports, Science and Technology of Japan (17390024). Part of this work was done at the Electron Microscope Laboratory, Kitasato University School of Medicine.

* To whom correspondence should be addressed: Tokyo University of Pharmacy and Life Science, Hachioji, Tokyo 192-0392, Japan. Phone: 81-426-76-5662. Fax: 81-426-46-5679. E-mail: nomizu@ps.toyaku.ac.jp.

‡ Tokyo University of Pharmacy and Life Science.

§ Division of Bioscience, Graduate School of Environmental Earth Science, Hokkaido University.

|| National Institutes of Health.

⊥ Kitasato University School of Medicine.

@ Division of Biological Sciences, Graduate School of Science, Hokkaido University.

10.1021/bi062097t CCC: $37.00
Published on Web 03/10/2007

containing peptide A208 (AASIKVAVSADR, mouse laminin α1 chain residues 2097−2108) forms amyloid-like fibrils composed of a cross-β conformation using Congo red staining, X-ray diffraction, infrared spectroscopy, and electron microscopy analyses (*16*). The IKVAV-containing sequence also promotes cell adhesion, neurite outgrowth, angiogenesis, collagenase IV production, and tumor growth (*17*−*21*). The IKVAV sequence promotes neurite outgrowth via interaction with a 110 kDa membrane-associated laminin-binding protein (*22*), which has been identified as a β-amyloid precursor protein (*23*, *24*). Interestingly, different amino acid substitutions of the IKVAV-containing peptide lost cell binding activity (*17*) or inhibit neurotoxicity (*25*). However, the functional relationship between the β-amyloid peptide and laminin-1 and laminin-derived peptides is not known.

In this paper, we identify amyloidogenic sequences among 60 biologically active peptides previously identified in laminin-1 (*26*−*30*). Congo red is a histological dye that binds to many amyloid-like proteins due to their extensive β-sheet structure. The absorption spectrum of the dye changes when it binds to amyloid (*31*). Congo red binding analysis is a quick method for assessing amyloid fibril formation (*32*−*34*). Several peptides were stained with Congo red and were further evaluated for their amyloidogenic properties by both X-ray diffraction and electron microscopic analysis. The amyloidogenic peptides were studied because of the relationship between fibril formation and biological activity. We report here on the finding of several additional amyloidogenic peptides from laminin-1 and describe key sequence elements responsible for the activity.

MATERIALS AND METHODS

Synthetic Peptides. All peptides were synthesized manually by the 9-fluorenylmethyloxycarbonyl (Fmoc)-based solid-phase methods with a C-terminal amide as described previously (*28*). The respective amino acids were condensed manually in a stepwise manner using diisopropylcarbodiimide *N*-hydroxybenzotriazole on a Rink amide resin (Novabiochem, San Diego, CA). The following side chain protecting groups were used: Asn, Cys, Gln, and His, trityl; Asp, Glu, Ser, Thr, and Tyr, *tert*-butyl; Arg, 2,2,5,7,8-pentamethylchroman-6-sulfonyl, and Lys, *tert*-butoxycarbonyl. Resulting protected peptide resins were deprotected and cleaved from the resin using a trifluoroacetic acid/thioanisole/*m*-cresol/ethanedithiol/H_2O mixture (80:5:5:5:5, by volume) at 20 °C for 3 h. Crude peptides were precipitated, washed with ethyl ether, and then purified by HPLC (using a Mightysil RP-18 column with a gradient of H_2O and acetonitrile containing 0.1% TFA). The purity and identity of the synthetic peptides were confirmed by analytical HPLC and by either fast atom bombardment or electrospray ionization mass spectroscopy. Mass spectroscopy was performed at the GC-MS & NMR Laboratory, Graduate School of Agriculture, Hokkaido University.

Congo Red Binding Analysis. A 100 μM stock solution of Congo red was prepared in phosphate-buffered saline (PBS) and 10% ethanol (*31*). Ethanol was added to prevent the formation of Congo red micelles. This Congo red stock solution was filtered three times using a 0.45 μm nylon membrane (Iwaki, Tokyo, Japan).

The peptide solutions in Milli-Q water (100 μL, 1.0 mg/mL) and the Congo red solution (100 μL, 100 μM in PBS) were mixed with 800 μL of PBS (1.25×) and incubated in disposable cuvettes for 24 h at room temperature. Absorption spectra were recorded from 300 to 700 nm using a U-560 UV−vis spectrophotometer (JASCO Co. Ltd., Tokyo, Japan). All absorption spectra result from the subtraction of the peptide scattering (absorption of peptide alone) from the Congo red spectral curve of the peptide.

Cells and Culture. HT-1080 human fibrosarcoma cells were maintained in Dulbecco's modified Eagle's medium (DMEM) containing 10% fetal bovine serum, 100 units/mL penicillin, and 100 μg/mL streptomycin (Invitrogen). PC12 cells (*35*) were maintained in DMEM/F12 containing 7.5% horse serum, 7.5% fetal bovine serum, 100 units/mL penicillin, and 100 μg/mL streptomycin (Invitrogen).

Cell Attachment Assay Using Peptide-Coated Plates. Attachment of cells to peptide-coated plates was assayed in 96-well plates (Immulon-2, DYNEX Technologies, Inc., Chantilly, VA). Plates were coated with various amounts of peptide in Milli-Q H_2O and dried overnight. The peptide-coated wells were blocked with 1% bovine serum albumin (BSA) (Sigma, St. Louis, MO) in DMEM (100 μL) for 1 h and then washed twice with DMEM containing 0.1% BSA. Cells (20 000 cells/100 μL), detached with trypsin and EDTA and resuspended in DMEM containing 0.1% BSA, were added to each well and incubated at 37 °C for 1 h in 5% CO_2. The attached cells were stained with a 0.2% crystal violet aqueous solution in 20% methanol for 10 min. After removal of the unattached cells, 1% SDS (200 μL) was used to dissolve the attached cells, and the optical density at 570 nm was measured in a model 550 microplate reader (Bio-Rad Laboratories, Hercules, CA).

Cell Attachment Assay Using Peptide-Conjugated Sepharose Beads. Peptides were coupled to cyanogen bromide (CNBr)-activated Sepharose 4B (Amersham Bioscience, Uppsala, Sweden) as described previously (*36*). Peptide solutions (200 μg, 1 mg/mL in Milli-Q H_2O) were mixed with the activated Sepharose beads (30 mg). Ethanolamine-coupled beads were prepared as a control. The amount of coupled peptide was determined by amino acid analysis (10−20 μmol of peptides per gram of Sepharose beads).

Attachment of cells to the peptide−Sepharose beads was assayed in 48-well plates (Iwaki). HT-1080 cells were detached as described above. The cells (10 000 cells/200 μL of DMEM containing 0.1% BSA) were incubated with 200 μL of the bead solution at 37 °C for 1 h in 5% CO_2. The cells attached to the beads were stained with a 0.2% crystal violet aqueous solution in 20% methanol for 10 min. After removal of the unattached cells, attached cells were analyzed under a microscope.

Neurite Outgrowth Assay. Peptides were dissolved in Milli-Q water at 1 mg/mL, kept at 4 °C for 1 week, and then used for the assay. For the neurite outgrowth assay, 16 mm diameter wells of a 24-well plate (Iwaki) were coated with various amounts of peptides and dried overnight. After the peptides had been coated, the plates were washed with DMEM/F12 (Invitrogen). PC12 cells were primed with 100 ng/mL nerve growth factor (NGF, Roche Diagnostics GmbH, Mannheim, Germany) for 24 h prior to the assay. The PC12 cells were then released from the dish by agitation, collected by centrifugation, allowed to recover in culture medium for 30 min at 37 °C in 5% CO_2, and then washed three times with DMEM/F12. Cells were resuspended in

DMEM/F12 containing 100 μg/mL transferrin (Sigma), 20 nM progesterone (Sigma), 30 nM Na_2SeO_3 (Wako, Osaka, Japan), 5 μg/mL insulin (Invitrogen), and 100 ng/mL NGF. The cells (20 000 cells/500 μL per well) were added to 24-well plates. After being incubated at 37 °C for 24 h in 5% CO_2, the cells were fixed with 20% formalin and then stained with 0.2% crystal violet. In each well (three fields), 100 cells were viewed, and the percent which had neurites that extended 2 times the cell diameter in length or longer was determined and averaged for each peptide amount that was tested.

Congo Red Staining and Polarized Light Microscopy. Peptides were dissolved in Milli-Q water at a concentration of 5 mg/mL, and the solution was pipetted onto a glass slide. After drying overnight, the precipitate was stained with a 1% aqueous solution of Congo red for 1 h. After being rinsed with pure acetone, the samples were dehydrated with 95% ethanol and 100% ethanol and then cleared with xylene. The specimens were mounted with a resin (malinol, Muto Pure Chemicals, Tokyo, Japan) and observed in a microscope (AX80, Olympus, Tokyo, Japan) either under bright field illumination or between crossed polars.

Electron Microscopy. The peptide solution (5 mg/mL) was diluted to 1:10−100 in Milli-Q water and applied onto a grid mesh with carbon-coated Formvar film. The specimen was then negatively stained with a 5% aqueous solution of uranyl acetate (A119, AG97, and Aβ 22−35) or 2% phospho tungstic acid (pH 7.0) (B133 and B160) and observed using a JEM-1200EX (JEOL, Tokyo, Japan) electron microscope at an acceleration voltage of 80 kV.

X-ray Diffraction. Peptides, dissolved in Milli-Q water (5 mg/mL), were packed into a siliconized-capillary glass tube (ϕ 0.3 mm, Verpackung ges, Berlin, Germany) and dried for 3 days in a wetting box at room temperature. Precipitate formed at the top of the capillary glass tube.

X-ray diffraction patterns were obtained at room temperature using Cu Kα (λ = 1.5418 Å) radiation from a MicroMax007 instrument (40 kV, 20 mA, Rigaku, Tokyo, Japan) with confocal Max-Flux mirrors. Data were collected on an R-AXIS IV^{++} diffractometer (Rigaku). The specimen−film distance was set at 250 mm, and the exposure time was 5 min. X-ray diffraction patterns were displayed and measured using CrystalClear (Rigaku).

RESULTS

Congo Red Staining Analysis. Previously, we screened biologically active sequences in laminin-1 using 673 synthetic peptides which cover the entire molecule and identified 60 cell adhesive peptides using peptide-coated plate and peptide-conjugated Sepharose bead assays (*26*−*30*) (Figure 1). Here, we have evaluated the effect of the 60-cell adhesive peptides on the Congo red absorption spectrum (Figure 2). When Congo red binds to amyloid structures, the absorption peak at 486 nm shifts to approximately 540 nm (*17*, *31*). A laminin peptide A208 (AASIKVAVSADR, laminin α1 chain residues 2097−2108) and Aβ 22−35 (EDVGSNKGAIIGLM, β-amyloid protein residues 22−35) were previously found to form amyloid-like fibrils in vitro (*17*, *37*) and were used here as positive controls (Figure 2). When the Congo red solution was incubated with the 60 active laminin-1 peptides at a concentration of 0.1 mg/mL

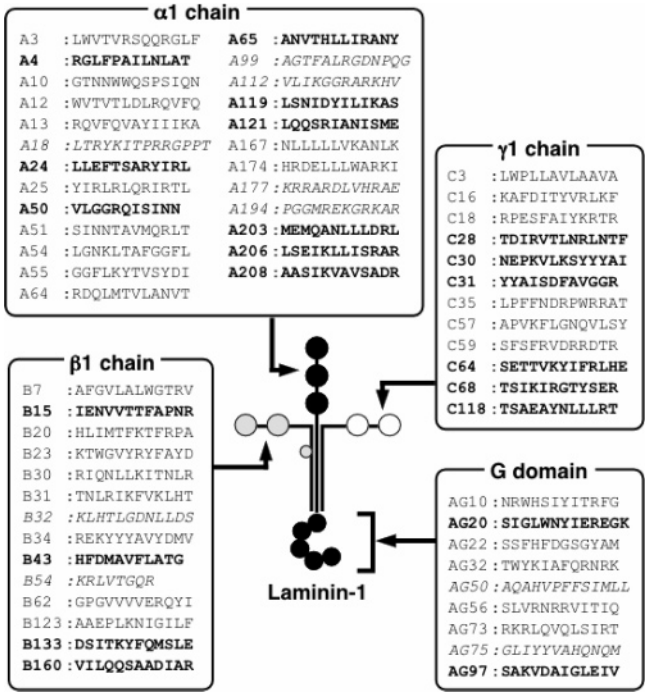

FIGURE 1: Localization of 60 cell adhesive peptides of laminin-1. Cell adhesive peptides identified previously are shown. Peptides are derived from mouse lamnin-1 (*25*−*28*). Twenty-one peptides exhibited cell attachment activity only in the peptide-coated plate assay (bold); nine peptides were active only in the peptide-conjugated Sepharose bead assay (italics), and 30 peptides promoted cell attachment in both assays (regular).

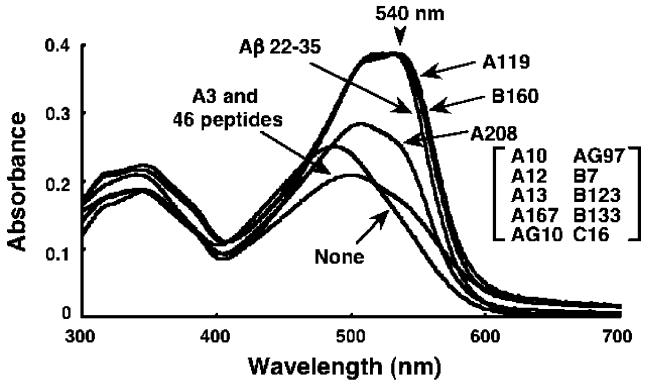

FIGURE 2: Absorption spectra of a Congo red solution in the presence of peptides. Peptide solubilized in Milli-Q water (100 μL, 1.0 mg/mL) and Congo red solution (100 μL, 100 μM in PBS) were mixed with 800 μL of PBS (1.25×), and the mixture was incubated for 24 h at room temperature. Absorption spectra were recorded from 300 to 700 nm. All absorption spectra result from subtraction of the peptide scattering (absorption of peptide alone) from the peptide incubated with the Congo red spectral curve.

for 24 h, 13 peptides caused a shift in the Congo red absorption peak (Figure 2 and Table 1). The absorption spectrum of Congo red was strongly affected by A119 and B160 peptides, and the response was comparable to that observed with Aβ 22−35 (Figure 2).

Biological Activity and Formation of Amyloid Structure. Recently, we found that an IKVAV-containing laminin-1-derived synthetic peptide, A208, forms amyloid-like fibrils composed of a cross-β conformation (*17*). We demonstrated that A208 exhibited cell attachment and neurite outgrowth activity only in the peptide-coated plate assay. Further, we demonstrate that the biological activity of A208 correlated

Table 1: Biological Activities of 13 Amyloidogenic Peptides Derived from Laminin-1

peptide	sequence	Congo red[a]	cell attachment[b] plate	cell attachment[b] bead	neurite outgrowth[b]
A10	GTNNWWQSPSIQN	+	++	++	+++
A12	WVTVTLDLRQVFQ	+	++	+	−
A13	RQVFQVAYIIIKA	+	+++	+++	+
A119	LSNIDYILIKAS	++	++	−	+
A167	NLLLLLVKANLK	+	++	++	−
A208	AASIKVAVSADR	+	+++	−	++
AG10	NRWHSYIYTRFG	+	+++	++	+
AG97	SAKVDAIGLEIV	+	+	−	+++
B7	AFGVLALWGTRV	+	+++	+++	−
B123	AAEPLKNIGILF	+	+	+	+
B133	DISTKYFQMSLE	+	+++	−	+++
B160	VILQQSAADIAR	++	+++	−	+
C16	KAFDITYVRLKF	+	+++	+++	+
AG73	RKRLQVQLSIRT	−	+++	+++	+++

[a] Peptides were incubated with Congo red solution, and absorption spectra were evaluated on the following subjective scale: ++, spectra comparable to that of Aβ 22−35; +, spectra comparable to that of A208; and −, no shift in the absorption peak. [b] Cell attachment and neurite outgrowth activities were scored on the following subjective scale: +++, activity comparable to that on AG73; ++, weak activity compared with that on AG73; +, very weak activity compared with that on AG73; and −, no activity.

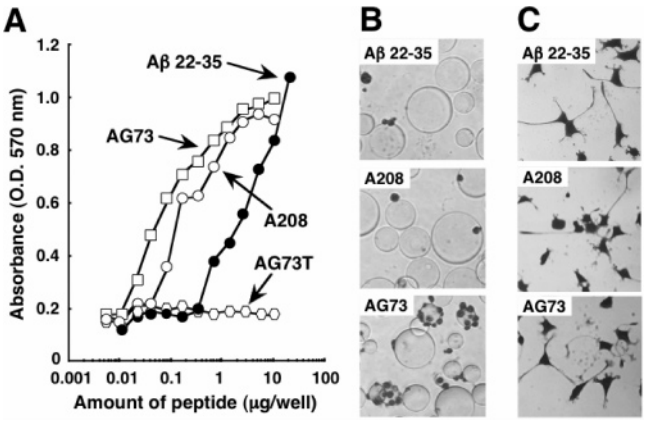

FIGURE 3: Cell attachment and neurite outgrowth activity. (A) Ninety six-well plates were coated with various amounts of peptides, and HT-1080 cells were added. After a 1 h incubation, the number of attached cells was assessed by crystal violet staining. Data are expressed as the mean of triplicate results. (B) HT-1080 cells were allowed to attach to peptide-conjugated Sepharose beads for 1 h and then stained with crystal violet. (C) Neurite outgrowth of PC12 cells on peptides. PC12 cells were cultured on peptides (50 μg/well) for 24 h and stained with crystal violet. AG73, which promotes cell attachment and PC12 neurite outgrowth (*25*, *39*), was used as a positive control. AG73T, which is a scrambled peptide of AG73, was used as a negative control.

with the ability to form amyloid-like fibrils using various A208 analogues (*17*). We, therefore, tested the Aβ 22−35 peptide for cell attachment and neurite outgrowth activity (Figure 3). We used AG73 (RKRLQVQLSIRT, mouse laminin α1 chain residues 2719−2730), previously identified as another active sequence in laminin-1 (*26*, *38*, *39*), as a positive control. AG73 promoted the cell attachment activity in both the peptide-coated plate and peptide-conjugated Sepharose bead assays (Figure 3A,B) and neurite outgrowth as described previously (Figure 3C) (*40*). Control scrambled AG73 peptide, AG73T, was inactive for cell adhesion. However, AG73 did not stain with Congo red (data not shown). The Aβ 22−35 peptide exhibited dose-dependent cell attachment activity in the peptide-coated plate assay but did not promote cell attachment in the peptide-conjugated Sepharose bead assay (Figure 3A,B). Aβ 22−35 also promoted neurite outgrowth (Figure 3C). The biological activity of the Aβ 22−35 peptide exhibited properties similar to those of peptide A208, suggesting that the biological activity of Aβ 22−35 may be related to the ability to form amyloid-like structures.

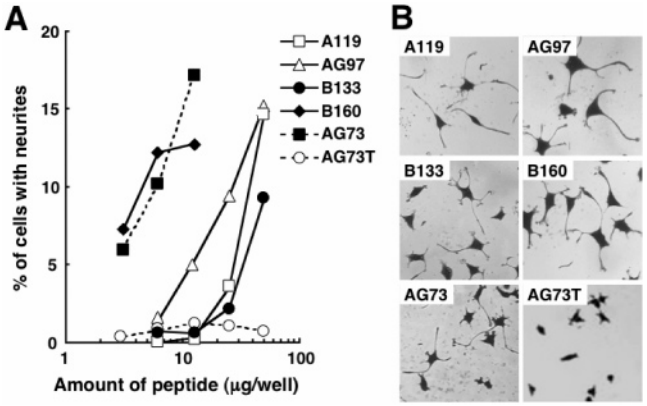

FIGURE 4: Neurite outgrowth of PC12 cells on peptides. (A) Various amounts of peptides were coated on 24-well plates. PC12 cells (20 000 cells/well) were seeded in the plates. After a 24 h incubation, cells were fixed and stained. The percentage of PC12 cells with neurites was determined as described in Materials and Methods. AG73 was used as a positive control, and AG73T was used as a negative control. (B) The PC12 cells were cultured on various peptides for 24 h and then stained with crystal violet. Peptides were coated on 24-well plates. A119, AG97, B133, and AG73T were at a concentration of 50 μg/well, and B160 and AG73 were at a concentration of 12.5 μg/well.

Neurite Outgrowth Activity of Peptides. We next evaluated the neurite outgrowth activity of the 13 peptides active in the Congo red assay (Table 1 and Figure 4). Peptide AG73 and the control scrambled peptide AG73T served as positive and negative controls. Ten peptides, including A10, A13, A119, A208, AG10, AG97, B123, B133, B160, and C16, exhibited neurite outgrowth activity. Five peptides, including A119, A208, AG97, B133, and B160, exhibited cell attachment activity only in the peptide-coated plate assay (Table 1). The five peptides also promoted neurite outgrowth in a dose-dependent manner (Figure 4) with activity comparable to that of Aβ 22−35. The rest of the peptides exhibited cell attachment activity in the both peptide-coated plate and peptide-conjugated Sepharose bead assays similar to that of AG73 (Table 1). On the basis of these results, we focused on the latter five peptides, including A119, A208, AG97, B133, and B160, for further evaluation of their amyloidogenicity.

Congo Red Staining and Polarized Microscopy of Peptides. Solutions of the five peptides (5 mg/mL) were pipetted onto slide glasses, dried, and stained with Congo red. The Aβ 22−35 peptide precipitate exhibited the red to green birefringence as expected (Figure 5I,J). The A208 peptide also exhibited birefringence as described previously (data not shown) (*17*). When the samples were observed under a polarizing microscope, three peptides (except B133 peptide) formed amyloid-like structures and exhibited birefringence, going from red to green (Figure 5). The B133 peptide exhibited very weak birefringence (Figure 5E,F). These results

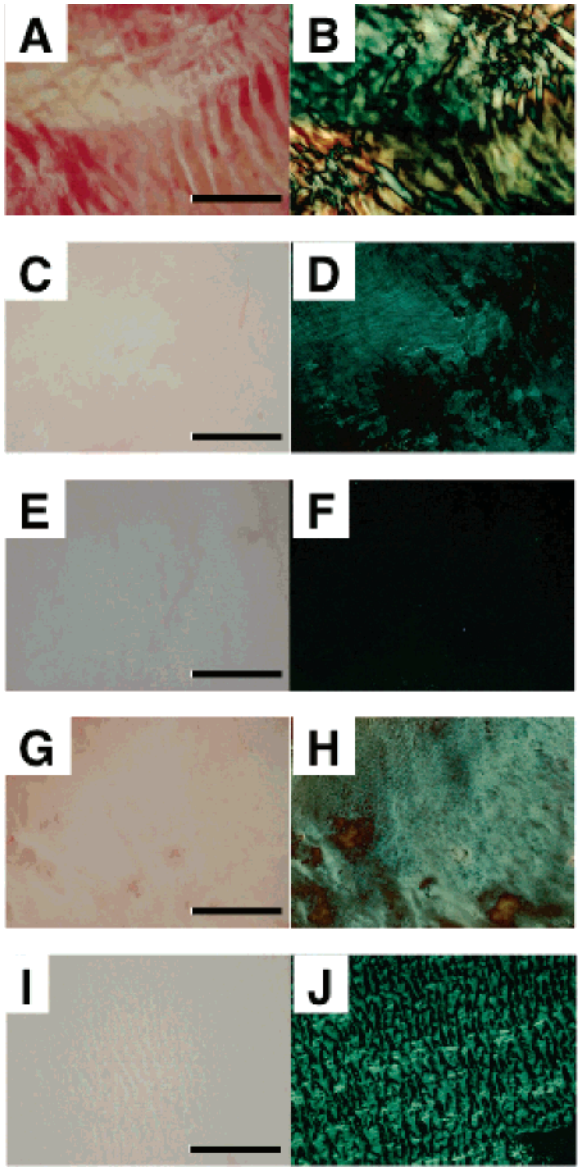

FIGURE 5: Photomicrographs of peptides stained with Congo red. Peptides in Milli-Q water (5 mg/mL) were pipetted onto a glass slide. After drying overnight, the precipitate was stained with a 1% aqueous solution of Congo red for 1 h. After being rinsed with pure acetone, the samples were dehydrated with 95% ethanol and with 100% ethanol and then cleared with xylene. The specimens were mounted with a resin and observed in a microscope either under bright field illumination (A, C, E, G, and I) or between crossed polars (B, D, F, H, and J): (A and B) A119, (C and D) AG97, (E and F) B133, (G and H) B160, and (I and J) Aβ 22−35. The scale bar is 100 μm.

further suggest that these peptides, A208, A119, AG97, and B160, form amyloid-like structures and significantly bind to Congo red.

Analysis of Amyloid-like Fibrils by Electron Microscopy. We next examined the ability of the four newly identified peptides to form amyloid-like fibrils. Peptide solutions (5 mg/mL) were diluted to 1:10−100 in Milli-Q water and analyzed by negative staining electron microscopy. Previously, A208 formed amyloid-like fibrils (*17*). Aβ 22−35 exhibited typical amyloid fibrils (Figure 6E), and all four peptides also formed fibrillar structures (Figure 6A−D). A119 exhibited long thin unbranching filaments similar to those of Aβ 22−35 (Figure 6A). AG97 exhibited filaments similar to those of A119, but the fibrils were shorter

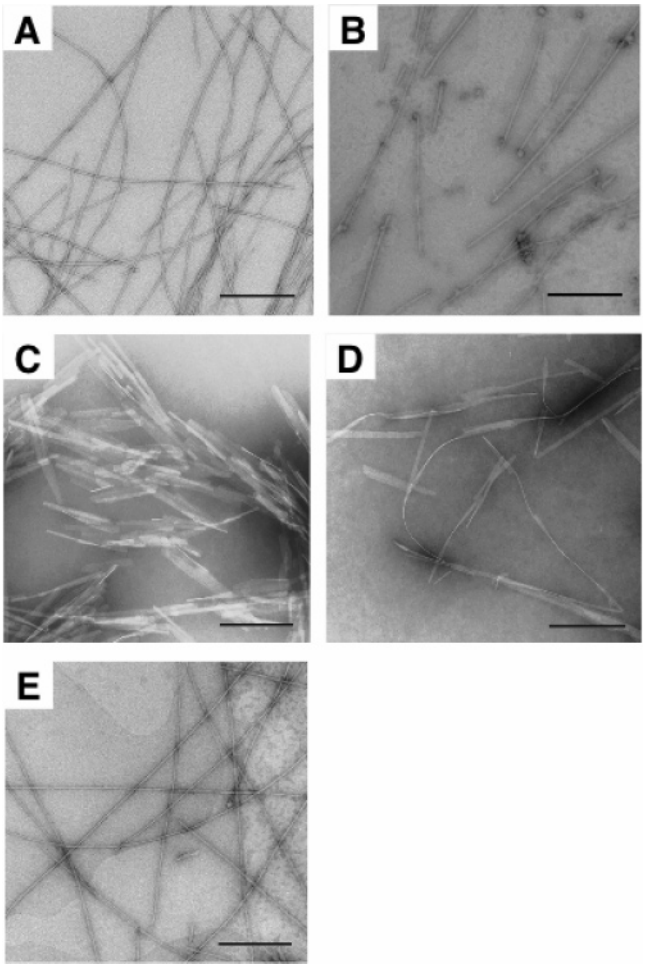

FIGURE 6: Electron micrographs of amyloid-like fibrils formed from peptides. The peptide solution (5 mg/mL) was diluted to 1:10−100 in Milli-Q water and applied to a grid mesh with carbon-coated Formvar film. The specimen was then negatively stained with either a 5% aqueous solution of uranyl acetate or 2% phospho tungstic acid (pH 7.0) and observed using an electron microscope: (A) A119, (B) AG97, (C) B133, (D) B160, and (E) Aβ 22−35. The scale bar is 200 nm.

(Figure 6B). The filaments of the B133 peptide were shorter and formed lateral aggregates (Figure 6C). The B160 peptide formed long ribbon-like fibrils (Figure 6D). These results suggest that these peptides self-assemble and form amyloid-like fibrils.

Secondary Structure Analysis of Peptides by X-ray Diffraction. Synthetic Aβ peptide-derived amyloid fibrils possess a cross-β conformation as determined by X-ray diffraction (*9*). When sufficient orientation of the fibrils can be obtained, characteristic orthogonal orientations of the respective X-ray reflections at 4.7 Å (from hydrogen bonding) and 10 Å (from intersheet packing) are observed (*41*). The X-ray diffraction pattern of the five peptides showed reflections that appear as rings due to the poor alignment of the fibrils (Figure 7). The A208 peptide exhibited a β-sheet reflection (*17*). A dominant sharp reflection at a position corresponding to 4.6−4.7 Å (from hydrogen bonding) was observed in all peptides (Figure 7). Aβ 22−35 exhibited two major well-oriented reflections at 4.7 and 10 Å, as expected (Figure 7E). The A119 peptide also exhibited two major well-oriented reflections at 4.7 and 11.5 Å (Figure 7A). These observed reflections at 10 and 11.5 Å suggest intersheet packing with a cross-β conformation in both of these peptides. These

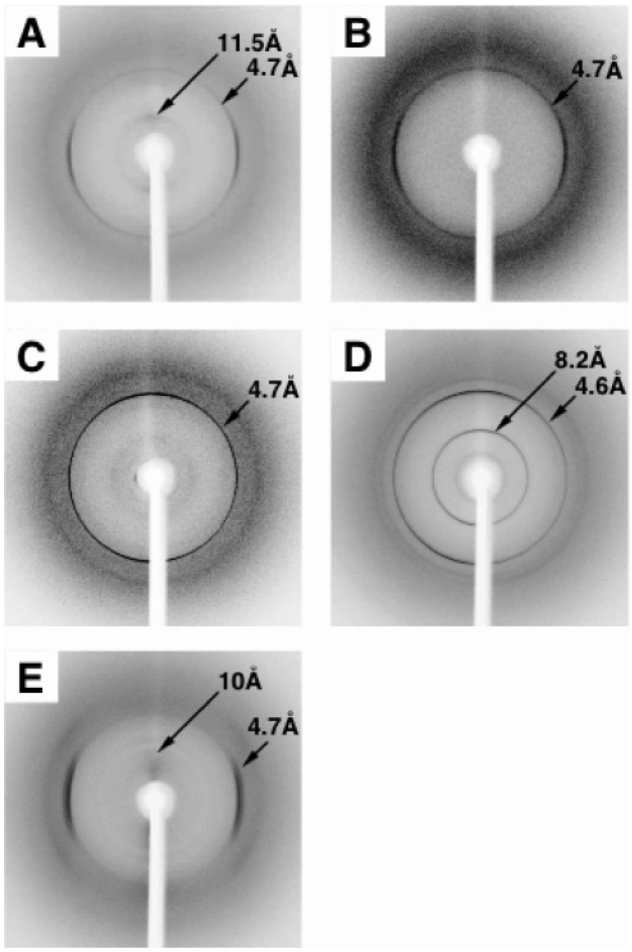

FIGURE 7: X-ray diffraction pattern of peptides. Peptides in Milli-Q water (5 mg/mL) were packed into a siliconized capillary glass tube and dried for 3 days in a wetting box at room temperature. Peptide A119 (A) exhibited typical a cross-β conformation with an orthogonal orientation of the 4.7 Å hydrogen bond and ~11.5 Å intersheet spacing that was observed for Aβ 22−35 (E). Peptides AG97 (B) and B133 (C) exhibited the reflection for a 4.7 Å hydrogen bond and reduction of the level of intersheet packing. Peptide B160 (D) has two major reflections of 4.7 and 8.2 Å. Due to the poor alignment of fibrils, those reflections appear as rings.

reflections are consistent with the cross-β conformation described for many amyloid fibrils (*9*, *41*, *42*). A similar, although not identical, cross-β pattern was recorded for the B160 peptide. B160 exhibited two reflections at 4.6 and 8.2 Å (Figure 7D). The reflection at 8.2 Å seems to be narrow for an intersheet distance, but this has not been characterized. AG97 and B133 exhibited reflections similar to those of A119, but the relative intensities of the intersheet reflections were significantly decreased (Figure 7B,C). The X-ray data suggest that the five peptides form a β-sheet conformation.

DISCUSSION

Amyloid fibril formation is generally related to diseases, including Alzheimer's disease, Parkinson's disease, type II diabetes, prion diseases, and systemic polyneuropathies (*1*, *2*). Amyloid fibrils are deposited in the basement membrane matrix of the brain (*43*). Laminin, type IV collagen, and heparan sulfate proteoglycans, which are the major components of the basement membrane, have been localized within the Alzheimer's plaques as punctate deposits (*10*, *11*). Laminins are degraded by proteases, including matrix metalloproteases (MMPs), in developmental and regenerative stages and diseases. Laminins and their fragments have been postulated to be involved in amyloid-related diseases (*13*, *14*). We previously found that a synthetic peptide from the laminin-1 sequence A208 (AASIKVAVSADR, mouse laminin α1 chain residues 2097−2108) forms amyloid-like fibrils and the ability to self-assemble correlates with the biological activity of the peptide (*17*).

In this paper, we identified four additional amyloidogenic peptides from laminin-1. Previously, 60 cell adhesive peptides were identified by the screening of 673 peptides covering the entire laminin-1 sequence using peptide-coated plate and a peptide-conjugated Sepharose bead assays (*26*−*30*). Thirty peptides promoted cell attachment in both assays; 21 peptides exhibited cell attachment activity only in the peptide-coated plate assay, and nine peptides were active only in the peptide-conjugated Sepharose bead assay. In this study, we used β-amyloid peptide Aβ 22−35 as a control. The Aβ 22−35 peptide exhibited cell attachment activity only in the peptide-coated plate assay and also promoted neurite outgrowth activity when coated on the plate. Twenty-one peptides, including A208, were active only in the peptide-coated plate assay and, thus, thought to share a similar property with the Aβ 22−35 peptide. We also evaluated the formation of amyloid-like structures by the 60 cell adhesive peptides using the Congo red assay. Thirteen peptides were active in the Congo red assay, suggesting that they could form amyloid-like structures. Taken together, five peptides (A119, A208, AG97, B133, and B160) were active in the Congo red assay and promoted cell attachment and neurite outgrowth only in the peptide-coated plate assay, suggesting that they formed amyloid-like structures with properties similar to those of Aβ 22−35.

Previously, we showed that peptide A208 formed long fibrils composed of β-sheet structures (*17*). In this study, A119, AG97, B133, and B160 were stained with Congo red and exhibited red to green birefringence. Using electron microscopic analysis, A119, AG97, B133, and B160 were observed as fibrillar structures. Further, X-ray diffraction data indicated that the fibrils of these four peptides were composed of β-sheet structures. These results strongly suggest that the five laminin-1-derived peptides self-assemble and form amyloid-like fibrils. The A119 peptide exhibited long thin unbranching filaments similar to that of a β-amyloid peptide, Aβ 22−35. X-ray data indicated that the A119 peptide had a well-oriented cross-β conformation that is consistent with the electron microscopic analysis. Taken together, the A119 peptide self-assembles into fibrils with typical properties of amyloid similar to those of Aβ 22−35. The AG97 peptide exhibited filaments similar to that of A119, but some reduction in length was observed. X-ray reflection of the AG97 peptide suggested a decrease in the level of intersheet packing. The short filaments of the AG97 peptide may also be due to a reduction in the intersheet packing ability. Peptides B133 and B160 exhibited ribbon-like fibrils. Peptide B133 filaments were shorter and formed lateral aggregates. This may be due to incomplete aggregation, and the ribbon structures may contain protofilaments. The very weak birefringence of the B133 peptide may be due to the properties of filaments. X-ray reflection of the B133 peptide indicated a reduction in the level of intersheet packing. This finding is consistent with the electron micros-

FIGURE 8: Alignment of amino acid sequences of amyloidogenic peptides. Sequences of Aβ 22−35 and amyloidogenic peptides from laminin-1 are listed, using the single-letter amino acid code. Basic amino acids (Arg and Lys) are boxed in white, and acidic amino acids (Asp and Glu) are boxed in black. A polar side chain (Ser and Thr) is boxed in gray, and β-branched hydrophobic amino acids (Ile and Val) are underlined.

copy results. There may be a relation between the morphological features of the filaments and the amyloidogenicity of peptides, but this has not yet been demonstrated.

Several studies on amyloid fibril formation suggest that the interaction of specific amino acid residues contributes to the formation and stabilization of the amyloid fibrils (*9*, *44*−*46*). The amino acid sequences of the five amyloidogenic peptides from laminin-1 and Aβ 22−35 were aligned (Figure 8). No clear consensus sequences were observed. All peptides have both basic and acidic amino acids, suggesting that charge interaction may be critical for fibril formation and/or stabilization of fibrils (*9*, *46*). It has been proposed that aromatic amino acids are an important part for amyloid fibrils (*45*), but three of the laminin peptides (except A119 and B133) have no aromatic residue. Aβ 22−35 also does not contain aromatic residues. Aromatic amino acids may not be essential for amyloid fibril formation but may accelerate fibril formation. Moreover, all five peptides and Aβ 22−35 contain polar side chain amino acids (Ser and Thr) and β-branched hydrophobic amino acids (Ile and Val). The β-branched amino acids (Ile and Val) may play a critical role in the self-assembly of the peptides into amyloid-like fibrils. Taken together, we conclude that both hydrophobic and electrostatic interactions may be necessary for the formation of amyloid-like fibrils.

Generally, it is thought that β-amyloid protein (Aβ) has a neurotoxic effect (*37*, *47*). Interestingly, we found that laminin-1-derived amyloidogenic peptides also have neurotoxicity that is on the same level as that of Aβ 22−35 (data not shown). However Aβ 22−35 or laminin-1-derived amyloidogenic peptides, when coated on a plastic plate as a substrate, promoted cell attachment and neurite outgrowth with PC12 cells (Figure 3). Previously, Koo et al. (*47*) reported that neurite outgrowth was enhanced by a combination of Aβ and laminin and minimally stimulated by Aβ alone. We do not know if the fibril structures of the amyloidogenic peptides may important for the biological activities in vivo. Recently, a relation among laminin, β-amyloid, and Alzheimer's disease has been reported (*10*−*14*, *23*, *24*, *43*). Laminin and its degraded fragments are present in Alzheimer's plaques (*14*), suggesting the association of laminin with the disease state. However, in vitro, laminin-1 interacts with β-amyloid proteins, inhibits the formation of amyloid fibrils, and reduces neurotoxicity (*14*, *15*). Snow et al. (*48*) reported that initial nonfibrillar plaques do not contain laminin, but in later stages, laminin is overexpressed by glial cells and accumulates in mature amyloid plaques. These results suggest that laminin is induced by glial cells to serve as a defensive neuroprotective role against the progression of the disease state. The laminin-1-derived peptides have inhibitory activity for neurotoxicity similar to that of laminin-1 in vitro except that they do not have inhibitory activity with respect to amyloid fibril formation. This difference may due to the lack of conformation or molecular size of the peptides, but our findings may help us understand and also may be useful tool for analyzing anti-neurotoxicity mechanisms at senile plaques in Alzheimer's disease.

Our data define potential active peptides on laminin that may function in vivo. Proteolytic fragments of laminins may contain activity that is cryptic in the intact molecule but which is revealed after proteolysis. For example, fragments of laminin-5 generated by MMP-9 induce cell migration and tumor metastasis (*49*). Cryptic active sites have been reported in a number of other molecules. For example, fragments of plasminogen and type XVIII collagen, designated angiostatin and endostatin, respectively, have important functions in regulating angiogenesis and tumor growth (*50*, *51*). It is possible that the active peptide fragments of laminin form amyloid-like fibrils and play a critical role in its biological activity. Degraded fragments of laminin may be involved in amyloid-related disease.

In this study, we identified several amyloidogenic sequences in the laminin-1 molecule. The amyloidogenic peptides form fibrils and promote cell attachment and neurite outgrowth. These peptides may useful in investigating the disease process and may lead to the development of peptide therapeutics.

ACKNOWLEDGMENT

We thank Dr. H. K. Kleinman (National Institute of Dental and Craniofacial Research) for encouragement and critical reading of the manuscript.

REFERENCES

1. Kelly, J. F. (1998) The alternative conformations of amyloidogenic proteins and their multi-step assembly pathways, *Curr. Opin. Struct. Biol. 8*, 101−106.
2. Rochet, J.-C., and Lansbury, P. T. (2000) Amyloid fibrillogenesis: Themes and variations, *Curr. Opin. Struct. Biol. 10*, 60−68.
3. Brange, J., Andersen, L., Laursen, E. D., Meyn, G., and Rasmussen, E. (1997) Toward understanding insulin fibrillation, *J. Pharm. Sci. 86*, 517−525.
4. Guijarro, J. I., Sunde, M., Jones, J. A., Campbell, I. D., and Dobson, C. M. (1998) Amyloid fibril formation by an SH3 domain, *Proc. Natl. Acad. Sci. U.S.A. 95*, 4224−4228.
5. Ohnishi, S., Koide, A., and Koide, S. (2000) Solution conformation and amyloid-like fibril formation of a polar peptide derived from a β-hairpin in the OspA single-layer β-sheet, *J. Mol. Biol. 301*, 477−480.
6. Sipe, J. D., and Cohen, A. S. (2000) History of the amyloid fibril, *J. Struct. Biol. 130*, 88−98.
7. Cooper, J. H. (1974) Selective amyloid staining as a function of amyloid composition and structure. Histochemical analysis of the alkaline Congo red, standardized toluidine blue, *Lab. Invest. 3*, 232−238.
8. Azriel, R., and Gazit, E. (2001) Analysis of the minimal amyloid-forming fragment of the islet amyloid polypeptide. An experimental support for the key role of the phenylalanine residue in amyloid formation, *J. Biol. Chem. 276*, 34156−34160.
9. Fraser, P. E., McLachlan, D. R., Surewicz, W. K., Mizzen, C. A., Snow, A. D., Nguyen, J. T., and Kirschner, D. A. (1994)

Conformation and fibrillogenesis of Alzheimer Aβ peptides with selected substitution of charged residues, *J. Mol. Biol. 244*, 64−73.
10. Perlmutter, L. S., Barron, E., Saperia, D., and Chui, H. C. (1991) Association between vascular basement membrane components and the lesions of Alzheimer's disease, *J. Neurosci. Res. 30*, 673−681.
11. Murtomaki, S., Risteli, J., Risteli, L., Koivisto, U. M., Johansson, S., and Liesi, P. (1992) Laminin and its neurite outgrowth-promoting domain in the brain in Alzheimer's disease and Down's syndrome patients, *J. Neurosci. Res. 32*, 261−273.
12. Colognato, H., and Yurchenco, P. D. (2000) Form and function: The laminin family of heterotrimers, *Dev. Dyn. 218*, 213−234.
13. Palu, E., and Liesi, P. (2002) Differential distribution of laminins in Alzheimer disease and normal human brain tissue, *J. Neurosci. Res. 69*, 243−256.
14. Castillo, G. M., Lukito, W., Peskind, E., Raskind, M., Kirschner, D. A., Yee, A. G., and Snow, A. D. (2000) Laminin inhibition of β-amyloid protein (Aβ) fibrillogenesis and identification of an Aβ binding site localized to the globular domain repeats on the laminin a chain, *J. Neurosci. Res. 62*, 451−462.
15. Morgan, C., and Inestrosa, N. C. (2001) Interactions of laminin with the amyloid β peptide. Implications for Alzheimer's disease, *Braz. J. Med. Biol. Res. 34*, 597−601.
16. Yamada, M., Kadoya, Y., Kasai, S., Kato, K., Mochizuki, M., Nishi, N., Watanabe, N., Kleinman, H. K., Yamada, Y., and Nomizu, M. (2002) Ile-Lys-Val-Ala-Val (IKVAV)-containing laminin α1 chain peptides form amyloid-like fibrils, *FEBS Lett. 530*, 48−52.
17. Tashiro, K., Sephel, G. C., Weeks, B., Sasaki, M., Martin, G. R., Kleinman, H. K., and Yamada, Y. (1989) A synthetic peptide containing the IKVAV sequence from the A chain of laminin mediates cell attachment, migration, and neurite outgrowth, *J. Biol. Chem. 264*, 16174−16182.
18. Grant, D. S., Tashiro, K., Segui-Real, B., Yamada, Y., Martin, G. R., and Kleinman, H. K. (1989) Two different laminin domains mediate the differentiation of human endothelial cells into capillary-like structures in vitro, *Cell 58*, 933−943.
19. Kanemoto, T., Reich, R., Royce, L., Greatorex, D., Adler, S. H., Shiraishi, N., Martin, G. R., Yamada, Y., and Kleinman, H. K. (1990) Identification of an amino acid sequence from the laminin A chain that stimulates metastasis and collagenase IV production, *Proc. Natl. Acad. Sci. U.S.A. 87*, 2279−2283.
20. Kibbey, M. C., Grant, D. S., and Kleinman, H. K. (1992) Role of the SIKVAV site of laminin in promotion of angiogenesis and tumor growth: An in vivo Matrigel model, *J. Natl. Cancer Inst. 84*, 1633−1638.
21. Nomizu, M., Utani, A., Shiraishi, N., Kibbey, M. C., Yamada, Y., and Roller, P. P. (1992) The all-D-configuration segment containing the IKVAV sequence of laminin A chain has similar activities to the all-L-peptide in vitro and in vivo, *J. Biol. Chem. 267*, 14118−14121.
22. Kleinman, H. K., Weeks, B. S., Cannon, F. B., Sweeney, T. M., Sephel, G. C., Clement, B., Zain, M., Olson, M. O. J., Jucker, M., and Burrous, B. A. (1991) Identification of a 110-kDa nonintegrin cell surface laminin-binding protein which recognizes an A chain neurite-promoting peptide, *Arch. Biochem. Biophys. 290*, 320−325.
23. Narindrasorasak, S., Lowery, D. E., Altman, R. A., Gonzalez-DeWhitt, P. A., Greenberg, B. D., and Kisilevsky, R. (1992) Characterization of high affinity binding between laminin and Alzheimer's disease amyloid precursor proteins, *Lab. Invest. 67*, 643−652.
24. Kibbey, M. C., Jucker, M., Weeks, B. S., Neve, R. L., Van Nostrand, W. E., and Kleinman, H. K. (1993) β-Amyloid precursor protein binds to the neurite-promoting IKVAV site of laminin, *Proc. Natl. Acad. Sci. U.S.A. 90*, 10150−10153.
25. Morgan, C., Bugueno, M. P., Garrido, J., and Inestrosa, N. C. (2002) Laminin affects polymerization, depolymerization and neurotoxicity of Aβ peptide, *Peptides 23*, 1229−1240.
26. Nomizu, M., Kim, W. H., Yamamura, K., Utani, A., Song, S. Y., Otaka, A., Roller, P. P., Kleinman, H. K., and Yamada, Y. (1995) Identification of cell binding sites in the laminin α1 chain carboxyl-terminal globular domain by systematic screening of synthetic peptides, *J. Biol. Chem. 270*, 20583−20590.
27. Nomizu, M., Kuratomi, Y., Song, S. Y., Ponce, L. M., Hoffman, M. P., Powell, S. K., Miyoshi, K., Otaka, A., Kleinman, H. K., and Yamada, Y. (1997) Identification of cell binding sequences in mouse laminin γ1 chain by systematic peptide screening, *J. Biol. Chem. 272*, 32198−32205.
28. Nomizu, M., Kuratomi, Y., Malinda, M. K., Song, S. Y., Miyoshi, K., Otaka, A., Powell, S. K., Hoffman, M. P., Kleinman, H. K., and Yamada, Y. (1998) Cell binding sequences in mouse laminin α1 chain, *J. Biol. Chem. 273*, 32491−32499.
29. Nomizu, M., Kuratomi, Y., Ponce, L. M., Song, S.-Y., Miyoshi, K., Otaka, A., Powell, S. K., Hoffman, M. P., Kleinman, H. K., and Yamada, Y. (2000) Cell adhesive sequences in mouse laminin β1 chain, *Arch. Biochem. Biophys. 378*, 311−320.
30. Suzuki, N., Ichikawa, N., Kasai, S., Yamada, M., Nishi, N., Morioka, H., Yamashita, H., Kitagawa, Y., Utani, A., Hoffman, M. P., and Nomizu, M. (2003) Syndecan binding sites in the laminin α1 chain G domain, *Biochemistry 42*, 12625−12633.
31. Klunk, W. E., Jacob, R. F., and Mason, R. P. (1999) Quantifying amyloid β-peptide (Aβ) aggregation using the Congo red-Aβ (CR-Aβ) spectrophotometric assay, *Anal. Biochem. 266*, 66−76.
32. Glenner, G. G., Eanes, E. D., and Page, D. L. (1972) The relation of the properties of Congo red-stained amyloid fibrils to the conformation, *J. Histochem. Cytochem. 20*, 821−826.
33. Luckey, M., Hernandez, J.-F., Arlaud, G., Forsyth, V. T., Ruigrok, R. W. H., and Mitraki, A. (2000) A peptide from the adenovirus fiber shaft forms amyloid-type fibrils, *FEBS Lett. 468*, 23−27.
34. Takahashi, T., Ueno, A., and Mihara, H. (1998) Design of a Peptide Undergoing $\alpha-\beta$ structural transition and amyloid fibrillogenesis by the introduction of a hydrophobic defect, *Chem.—Eur. J. 4*, 2475−2484.
35. Greene, L. A., and Tischler, A. S. (1976) Establishment of a noradrenergic clonal line of rat adrenal pheochromocytoma cells which respond to nerve growth factor, *Proc. Natl. Acad. Sci. U.S.A. 73*, 2424−2428.
36. Nomizu, M., Song, S. Y., Kuratomi, Y., Tanaka, M., Kim, W. H., Kleinman, H. K., and Yamada, Y. (1996) Active peptides from the carboxyl-terminal globular domain of laminin α2 and *Drosophila* α chains, *FEBS Lett. 396*, 37−42.
37. Takadera, T., Sakura, N., Mohri, T., and Hashimoto, T. (1993) Toxic effect of a β-amyloid peptide (β 22−35) on the hippocampal neuron and its prevention, *Neurosci. Lett. 161*, 41−44.
38. Hoffman, M. P., Nomizu, M., Roque, E., Lee, S., Jung, D. W., Yamada, Y., and Kleinman, H. K. (1998) Laminin-1 and laminin-2 G-domain synthetic peptides bind syndecan-1 and are involved in acinar formation of a human submandibular gland cell line, *J. Biol. Chem. 273*, 28633−28641.
39. Hoffman, M. P., Engbring, J. A., Nielsen, P. K., Vargas, J., Steinberg, Z., Karmand, A. J., Nomizu, M., Yamada, Y., and Kleinman, H. K. (2001) Cell type-specific differences in glycosaminoglycans modulate the biological activity of a heparin-binding peptide (RKRLQVQLSIRT) from the G domain of the laminin α1 chain, *J. Biol. Chem. 276*, 22077−22085.
40. Richard, B. L., Nomizu, M., Yamada, Y., and Kleinman, H. K. (1996) Identification of synthetic peptides derived from laminin α1 and α2 chains with cell type specificity for neurite outgrowth, *Exp. Cell Res. 228*, 98−105.
41. Kirschner, D. A., Abraham, C., and Selkoe, D. J. (1986) X-ray diffraction from intraneuronal paired helical filaments and extraneuronal amyloid fibers in Alzheimer disease indicates cross-β conformation, *Proc. Natl. Acad. Sci. U.S.A. 83*, 503−507.
42. Jaikaran, E. T., Higham, C. E., Serpell, L. C., Zurdo, J., Gross, M., Clark, A., and Fraser, P. E. (2001) Identification of a novel human islet amyloid polypeptide β-sheet domain and factors influencing fibrillogenesis, *J. Mol. Biol. 308*, 515−525.
43. Inoue, S., Kuroiwa, M., and Kisilevsky, R. (1999) Basement membranes, microfibrils and β amyloid fibrillogenesis in Alzheimer's disease: High resolution ultrastructural findings, *Brain Res. Brain Res. Rev. 29*, 218−231.
44. Hilbich, C., Kisters-Woike, B., Reed, J., Masters, C. L., and Beyreuther, K. (1992) Substitutions of hydrophobic amino acids reduce the amyloidogenicity of Alzheimer's disease β A4 peptides, *J. Mol. Biol. 228*, 460−473.
45. Reches, M., Porat, Y., and Gazit, E. (2002) Amyloid fibril formation by pentapeptide and tetrapeptide fragments of human calcitonin, *J. Biol. Chem. 277*, 35475−35480.
46. Tjernberg, L., Hosia, W., Bark, N., Thyberg, J., and Johansson, J. (2002) Charge attraction and β propensity are necessary for

amyloid fibril formation from tetrapeptides, *J. Biol. Chem. 277*, 43243−43246.
47. Koo, E. H., Park, L., and Selkoe, D. J. (1993) Amyloid β-protein as a substrate interacts with extracellular matrix to promote neurite outgrowth, *Proc. Natl. Acad. Sci. U.S.A. 90*, 4748−4752.
48. Snow, A. D., Mar, H., Nochlin, D., Sekiguchi, R. T., Kimata, K., Koike, Y., and Wight, T. N. (1990) Early accumulation of heparan sulfate in neurons and in the β-amyloid protein-containing lesions of Alzheimer's disease and Down's syndrome, *Am. J. Pathol. 137* (5), 1253−1270.
49. Giannelli, G., Falk-Marzillier, J., Schiraldi, O., Stetler-Stevenson, W. G., and Quaranta, V. (1997) Induction of cell migration by matrix metalloprotease-2 cleavage of laminin-5, *Science 277*, 225−228.
50. O'Reilly, M. S., Holmgren, L., Shing, Y., Chen, C., Rosenthal, R. A., Moses, M., Lane, W. S., Cao, Y., Sage, E. H., and Folkman, J. (1994) Angiostatin: A novel angiogenesis inhibitor that mediates the suppression of metastases by a Lewis lung carcinoma, *Cell 79*, 315−328.
51. O'Reilly, M. S., Boehm, T., Shing, Y., Fukai, N., Vasios, G., Lane, W. S., Flynn, E., Birkhead, J. R., Olsen, B. R., and Folkman, J. (1997) Endostatin: An endogenous inhibitor of angiogenesis and tumor growth, *Cell 88*, 277−285.

BI062097T